

# Investigation, Design, and Evaluation of a Riemann Pump in GaN Technology

Markus Weiß, Christian Friesicke, Rüdiger Quay, and Oliver Ambacher

Fraunhofer Institute for Applied Solid State Physics

Freiburg, Germany

[markus.weiss@iaf-extern.fraunhofer.de](mailto:markus.weiss@iaf-extern.fraunhofer.de)

**Abstract**—A novel architecture for radio-frequency digital-to-analog converters (RF DACs) is investigated that improves the signal-to-noise ratio (SNR) of conventional converter concepts. The presented concept results in an arbitrary waveform generator that is capable to provide several watts of output power. Further, the high electron mobility transistor (HEMT) technology provides high switching frequencies to ensure an oversampling ratio of 5 for a wide baseband bandwidth. The utilization of gallium nitride (GaN) enables to design a one-chip solution of a RF DAC co-integrated with a power amplifier (PA), which is named Riemann Pump. The Riemann Pump, which is controlled with a digital bit-stream, is based on the current steering topology and provides the possibility to synthesize arbitrary waveforms. A two-bit RF DAC designed with multiple monolithic microwave integrated circuits (MMICs) proofs the feasibility to generate arbitrary waveforms. Measurement results yield triangular signals with a baseband frequency of 100 MHz for an input-control data rate of 200 Mbps.

**Index Terms**—AWG, DAC, transmitter architecture.

## I. INTRODUCTION

THE immense demand for high data rates in mobile communication leads researchers to investigate new architectures to improve the conventional concepts. One concept that improves the performance is the Riemann Pump [1]. The aim to develop a Riemann Pump in GaN technology is to generate a high power modulated microwave signal, which is suitable for the next generation of mobile communication. The possibility to cover a frequency range from DC to 6 GHz enables this architecture to operate with all common mobile communication standards. The advantage of GaN is to switch high power at high frequencies as conventional CMOS switches are limited in power. As the power consumption of GaN HEMTs exceeds the limits for mobile devices the presented architecture is suitable for base station transmitters.

The presented concept of the Riemann Pump improves the SNR compared to conventional pulse-code modulation (PCM) converters. A PCM converter improves the SNR by 5 to 7 dB for every one-bit increase of resolution while the Riemann conversion improves it by 5 to 10 dB [2]. Every doubling of the

Manuscript received XXX YY, ZZZZ; revised XXX YY, ZZZZ; accepted XXX YY, ZZZZ. Date of publication Month XX, ZZZZ; date of current version XXX YY, ZZZZ.

M. Weiß, C. Friesicke, R. Quay and O. Ambacher are with the Fraunhofer Institute for Applied Solid-State Physics (IAF), 79108 Freiburg, Germany.

Color versions of one or more of the figures in this letter are available online at <http://ieeexplore.ieee.org>.

Digital Object Identifier XXXXXXXX

oversampling ratio (OSR), which is defined as  $\text{OSR} = \frac{f_{\text{sampling}}}{2f_{\text{signal,max}}}$ , improves the SNR of a PCM converter by 3 dB while the Riemann conversion improves it by 9 dB. The mathematical approximation for the SNR of the Riemann Pump is given in Equation 1. For further details and the derivation see [2].

$$\text{SNR}_{\text{dB}} \approx 6.02N + 9.03r - 7.78 + 10 \log \left( 1 - \frac{1}{2^{N-1}} + \frac{1}{2^{2N}} \right) \quad (1)$$

The factor  $N$  represents the number of bits used for the resolution, while  $r$  is the binary logarithm of the OSR.

This paper presents the first realization of a Riemann Pump in GaN technology. The new concept of the Riemann Pump shows the feasibility to improve the data rate. A circuit is devised and designed in Chapter II based on the presented idea. Chapter III covers the implementation and assembly of a first Riemann Pump demonstrator. In Chapter IV measurement results verify the feasibility of the concept by the generation of a triangular signal, which is representative for any signal waveform. Chapter V summarizes the paper and give a short outlook for future work.

## II. CONCEPT OF THE RIEMANN PUMP CIRCUIT

In this section a RF DAC is described which is derived from the concept of a charge pump. The digital-to-analog conversion is based on the current steering topology and pumps charges into a capacitive output load. The current into the capacitive load is integrated over time to form the resulting voltage. Hence, this custom charge pump is named after the inventor of the Riemann integral, Bernhard Riemann. Figure 1 shows the schematic of the Riemann Pump, where the single stages are cascaded in parallel. The current-drive capability of the power transistors in parallel is increased linearly with the power of 2 to ensure the correct encoding. The digital driver circuit is marked with dashed lines and is necessary for each single stage cascaded in parallel. An implemented power amplifier, serving as the output load, enables to reduce the number of external components in the radio-frequency front-end (RFFE). The capacitive input impedance of the power amplifier makes it suitable for this concept. The driver circuit enables to control the power transistors, which are intended to be a voltage-controlled current sources, with a digital bit stream. Based

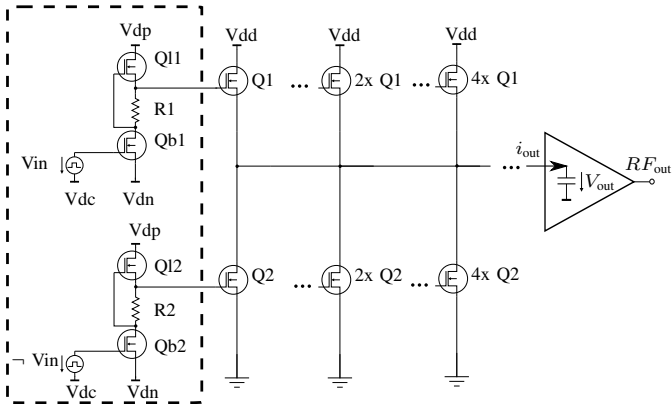


Fig. 1. Schematic of the Riemann Pump. Marked on the left side is the driver circuit. The push-pull stages are connected in parallel.

on a charge pump the resulting output voltage at the load is defined as:

$$V_{\text{out}} = \frac{1}{C_{\text{out}}} \int_0^t i_{\text{out}}(\tau) d\tau. \quad (2)$$

Equation 2 states the dependence of the voltage through the current and time at the output load. This technique makes it possible to synthesize arbitrary voltage waveforms at the PA by varying the current. Absolutely essential to convert digital input data into a defined analog output signal is to establish a defined set of current amplitudes which charge and discharge the output capacitance, here the input impedance of the PA. For a good approximation of the synthesized signal, a high sampling frequency as well as stable current sources are needed. In Fig. 2(a) eight different slopes represent the change of the output voltage for a given sampling interval. These eight slopes correspond to a three-bit resolution of the DAC. Figure 2(b) illustrates an example of a synthesized output signal using these slopes. The solid black line represents the desired output

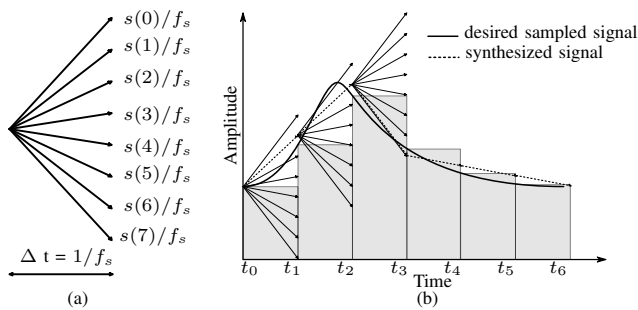


Fig. 2. (a) Representation of relative slopes and (b) signal generation with riemann code.

signal to be synthesized by the Riemann Pump. For each sampling point, the slope that minimizes the error between the sampled desired and the synthesized signal is chosen. As eight different slopes are generated, it corresponds with a three-bit resolution of the RF DAC enabling an encoding of each slope with a digital bit stream. It is possible to control the output signal with a digital input stream representing the sequence of slopes to synthesize the signal. In order to generate eight different currents the concept of a charge pump in a push-pull

configuration is used. The high-side transistors contribute to an increase of the output signal while the low-side transistors decrease the amplitude of the output signal. Mandatory for the correct functioning of the push-pull configuration is a digital driver circuit to ensure a proper switching of the high-side transistors. To prevent a signal delay caused by this driver circuit, this driver is also used for the low-side transistor.

### III. IMPLEMENTATION AND ASSEMBLY OF A DEMONSTRATOR

To the best of the author's knowledge, the first ever built demonstrator in GaN technology is presented. To ensure a feasible measurement setup, the RF DAC is realized with a two-bit resolution which is sufficient to prove the concept. For the digital switching of the GaN power transistors a MMIC is used which has already implemented a proper driver circuit. These MMICs are designed and fabricated in the  $0.25\text{ }\mu\text{m}$  AlGaN/GaN HEMT technology by Fraunhofer IAF [3]. Figure 3 (a) illustrates the schematic where the grey painted areas represent a single MMIC. In Fig. 3(b) the layout of the realized demonstrator is shown. The green rectangles represent off-

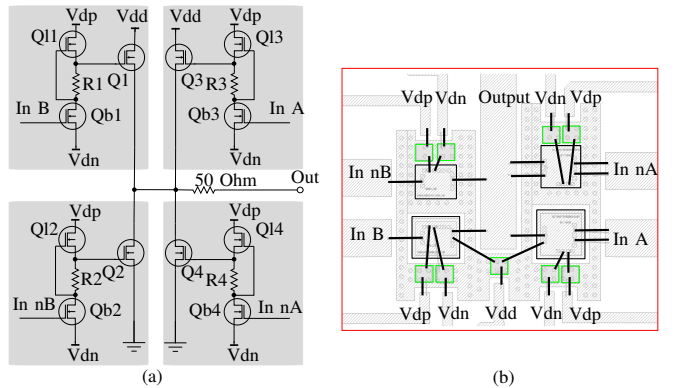


Fig. 3. (a) Schematic of assembly; the used MMICs are highlighted in grey. (b) Assembled demonstrator layout.

chip bypass capacitors, and the black rectangles are the used MMICs. Each MMIC, consisting of the grey highlighted circuit in Figure 3 (a), have got a via to the backside at the power transistors source potential. In fact of this via and the backside metallization it is necessary to isolate the MMICs for the high-side transistors Q1 and Q3. This isolation is realized by an isolated pad on the substrate, which induces a critical heat transfer. In order to reduce the impact of phase delays of the signal the input and output lines as well as the bond wires are of the same length.

The first Riemann Pump in GaN technology is shown in Figure 4. A close-up of assembled MMICs is shown in Figure 4 (a) according to the layout in Figure 3(b). This close-up is highlighted in the photography of the demonstrator in Figure 4 (b). The demonstrator is of the size  $50 \times 60\text{ mm}^2$ , has four digital input and one analog output line and DC supply connectors with decoupling network. The analog output is at the top middle while the other four signal paths are the digital inputs.

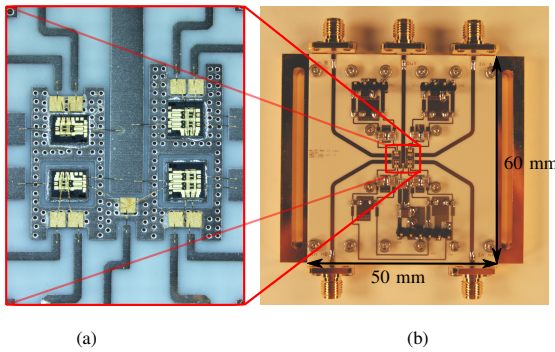


Fig. 4. (a) Close-up of assembled MMICs, (b) realized demonstrator.

#### IV. TIME-DOMAIN MEASUREMENT OF SYNTHESIZED OUTPUT SIGNAL

To prove that the built demonstrator can convert digital input streams into an analog output signal, a time-domain measurement is performed. A custom control and measurement setup was applied to ensure excitation of the device under test (DUT) with correct amplitude and phase. Four input signals are applied by an arbitrary waveform generator (AWG) (Keysight M8195A) to represent the digital data stream. These signals had to be amplified by a broadband pre-amplifier and shifted in the DC offset with bias tees to ensure proper switching of the transistors Qb1, Qb2, Qb3 and Qb4 at the input. First of all, a stability analysis is performed to ensure that the DUT does not oscillate. Further, both high-side transistors (Q1, Q3) are controlled with an in-phase signal illustrated in Figure 5(a) (grey), while the inverse signal (black) is applied to both low-side transistors (Q2, Q4). This differential digital input stream is generated by the AWG for a data rate of 200 Mbps in the time-domain. The DUT is loaded with a  $50\Omega$  resistor and is controlled by this input signal, which leads to the output signal shown in Figure 5 (b). As expected for a push-pull signal shown in Figure 5 (b).

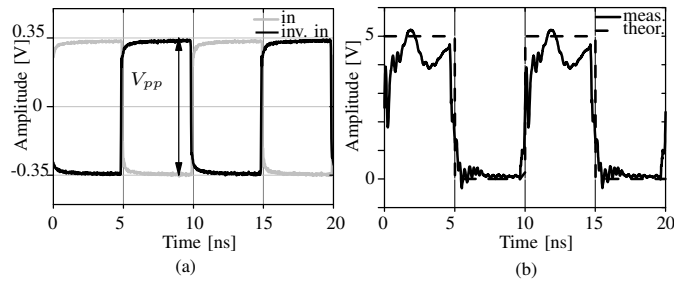


Fig. 5. (a) Differential input control signal and (b) corresponding output signal; theoretical signal (dashed), measured signal (solid).

measurement the output signal switches between  $V_{dd}$  (5V) and GND (0V). The dashed line represents the output of an ideal switch while the solid line shows the measured output signal of the DUT. To show the feasibility to synthesize different output signals it is necessary to generate different currents which are integrated at a capacitor, as mentioned in Chapter II. Therefore the resistive load is replaced by a capacitive load, representing the capacitive input impedance characteristic of a PA. In-phase switching of both high-side and low-side transistors led to the

results shown in Figure 6 (b). Here the capacitor is charged with the maximum available current as both high-side transistors simultaneously drive current to the load, hence the biggest slope is chosen. Encoding the biggest slope with the bit-sequence "00" the corresponding most negative slope is "11" while "01" and "10" contribute to the smaller slopes in between. In order to select the slope  $i_0$  both high-side as well as both low-side transistors are driven with anti-phase signals. The slope  $i_0$  is illustrated in Figure 6(a) while the bigger slope  $3i_0$  is shown in (b).

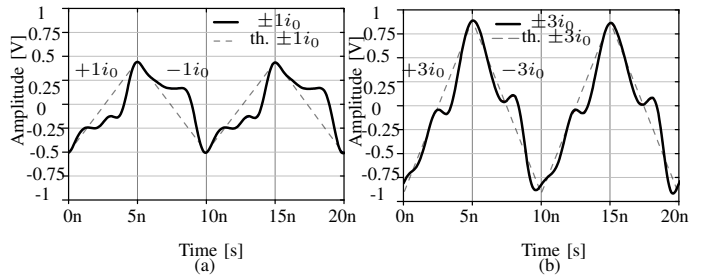


Fig. 6. ideal slope (dashed); measurement (solid). Slope of (a)  $\pm 1i_0$  and (b)  $\pm 3i_0$ .

The notation of both figures is the same, the solid black line represents the measured time-domain signal for the frequency of 100 MHz, while the dashed line represents the ideal signal waveform.

#### V. CONCLUSION

A first prototype of a Riemann Pump in GaN technology is presented to validate the concept of this current steering topology. The measurement results show the feasibility of synthesizing arbitrary waveforms at 100 MHz. The potential of the chosen technology promises to cover even higher frequencies to satisfy the condition for the new mobile communication standards.

#### ACKNOWLEDGEMENT

The authors would like to thank Dirk Meder at Fraunhofer IAF for the assistance with the assembly process.

#### REFERENCES

- [1] Y. Veyrac, F. Rivet, Y. Deval, D. Dallet, P. Garrec, and R. Montigny, "The Riemann Pump: a Concurrent Transmitter in Gan Technology," in *21st IEEE International Conference on Electronics and Circuits and Systems (ICECS)*, 2014, pp. 594 – 597.
- [2] ——, "A 65 nm CMOS DAC Based on a Differentiating Arbitrary Waveform Generator Architecture for 5G Handset Transmitter," in *IEEE TRANS. CIRCUITS SYST. II, EXPRESS BRIEFS*, vol. 63, no. 1, 2016, pp. 104 – 108.
- [3] S. Maroldt, C. Haupt, R. Kiefer, W. Bronner, S. Mueller, W. Benz, R. Quay, and O. Ambacher, "High Efficiency Digital GaN MMIC Power Amplifiers for Future Switch-Mode Based Mobile Communication Systems," in *2009 Annual IEEE Compound Semiconductor Integrated Circuit Symposium*, Oct 2009, pp. 1-4.
- [4] Y. Deval, F. Rivet, and Y. Veyrac, "Design by Mathematics of Full Software Radio circuits and systems: methodology and application to 5G standard," in *EUROPEAN MICROWAVE WEEK*, 2015.
- [5] S. Maroldt, P. Brückner, R. Quay, and O. Ambacher, "A microwave high-power GaN transistor with highly-integrated active digital switch-mode driver circuit," in *IEEE MTT-S International Microwave Symposium (IMS2014)*, 2014, pp. 1 – 4.